



Universiteit  
Leiden  
The Netherlands

**Selective chemical shift assignment of B800 and B850 bacteriochlorophylls in uniformly [C-13,N-15]-labeled light-harvesting complexes by solid-state NMR spectroscopy at ultra-high magnetic field**

Gammeren, A.J. van; Buda, F.; Hulsbergen, F.B.; Kiihne, S.; Hollander, J.G.; Egorova-Zachernyuk, T.A.; ... ; Groot, H.J.M. de

**Citation**

Gammeren, A. J. van, Buda, F., Hulsbergen, F. B., Kiihne, S., Hollander, J. G., Egorova-Zachernyuk, T. A., ... Groot, H. J. M. de. (2005). Selective chemical shift assignment of B800 and B850 bacteriochlorophylls in uniformly [C-13,N-15]-labeled light-harvesting complexes by solid-state NMR spectroscopy at ultra-high magnetic field. *Journal Of The American Chemical Society*, 127(9), 3213-3219. doi:10.1021/ja044215a

Version: Publisher's Version

License: [Licensed under Article 25fa Copyright Act/Law \(Amendment Taverne\)](#)

Downloaded from: <https://hdl.handle.net/1887/3458749>

**Note:** To cite this publication please use the final published version (if applicable).

## Selective Chemical Shift Assignment of B800 and B850 Bacteriochlorophylls in Uniformly [ $^{13}\text{C}$ , $^{15}\text{N}$ ]-Labeled Light-Harvesting Complexes by Solid-State NMR Spectroscopy at Ultra-High Magnetic Field

Adriaan J. van Gammeren,<sup>†</sup> Francesco Buda,<sup>†</sup> Frans B. Hulsbergen,<sup>†</sup> Suzanne Kiihne,<sup>†</sup> Johan G. Hollander,<sup>†</sup> Tatjana A. Egorova-Zachernyuk,<sup>†</sup> Niall J. Fraser,<sup>‡</sup> Richard J. Cogdell,<sup>‡</sup> and Huub J. M. de Groot<sup>\*†</sup>

Contribution from the Leiden Institute of Chemistry, Gorlaeus Laboratoria, Leiden University, P.O. Box 9502, 2300 RA Leiden, The Netherlands, and Division of Biochemistry and Molecular Biology, Institute of Biomedical and Life Sciences, University of Glasgow, Glasgow G12 8QQ, U.K.

Received September 23, 2004; E-mail: ssnmr@chem.leidenuniv.nl

**Abstract:** The electronic ground states of the bacteriochlorophyll a type B800 and type B850 in the light-harvesting 2 complex of *Rhodospseudomonas acidophila* strain 10050 have been characterized by magic angle spinning (MAS) dipolar  $^{13}\text{C}$ – $^{13}\text{C}$  correlation NMR spectroscopy. Uniformly [ $^{13}\text{C}$ , $^{15}\text{N}$ ] enriched light-harvesting 2 (LH2) complexes were prepared biosynthetically, while [ $^{13}\text{C}$ , $^{15}\text{N}$ ]-B800 LH2 complexes were obtained after reconstitution of apoprotein with uniformly [ $^{13}\text{C}$ , $^{15}\text{N}$ ]-enriched bacteriochlorophyll cofactors. Extensive sets of isotropic  $^{13}\text{C}$  NMR chemical shifts were obtained for each bacteriochlorin ring species in the LH2 protein.  $^{13}\text{C}$  isotropic shifts in the protein have been compared to the corresponding shifts of monomeric BChl *a* dissolved in acetone- $d_6$ . Density functional theory calculations were performed to estimate ring current effects induced by adjacent cofactors. By correction for the ring current shifts, the  $^{13}\text{C}$  shift effects due to the interactions with the protein matrix were resolved. The chemical shift changes provide a clear evidence for a global electronic effect on the B800 and B850 macrocycles, which is attributed to the dielectrics of the protein environment, in contrast with local effects due to interaction with specific amino acid residues. Considerable shifts of  $-6.2 < \Delta\sigma < +5.8$  ppm are detected for  $^{13}\text{C}$  nuclei in both the B800 and the B850 bacteriochlorin rings. Because the shift effects for the B800 and B850 are similar, the polarization of the electronic ground states induced by the protein environment is comparable for both cofactors and corresponds with a red shift of  $\sim 30$  nm relative to the monomeric BChl dissolved in acetone- $d_6$ . The electronic coupling between the B850 cofactors due to macrocycle overlap is the predominant mechanism behind the additional red shift in the B850.

### Introduction

Bacteriochlorophylls (BChl) and carotenoids are the main light-absorbing cofactors in purple bacteria. They are noncovalently bound to two types of integral membrane proteins, the photosynthetic reaction centers and light-harvesting or antenna complexes.<sup>1</sup> The antenna cofactors absorb photons, yielding an excitation that is transferred via excitonic coupling and Förster energy transfer from the peripheral light-harvesting complexes to the reaction center where the charge separation takes place.<sup>2</sup>

Bacterial photosynthetic complexes can be isolated in relatively large quantities. They can be stabilized with a small amount of detergent. In this study, we focus on resolving the electronic structure of the BChls in the bacterial photosynthetic

light-harvesting 2 (LH2) complex from *Rhodospseudomonas (Rps.) acidophila* strain 10050 by magic angle spinning (MAS) NMR. Detailed structural data have been obtained by X-ray crystallography for two bacterial photosynthetic LH2 complexes, from *Rps. acidophila* and from *Rhodospirillum molischianum*.<sup>3,4</sup> The LH2 intrinsic membrane protein of *Rps. acidophila* is a circular aggregate complex containing nine identical monomeric units that consist of two membrane spanning helices, the  $\alpha$ -subunit with 53 residues and the  $\beta$ -subunit with 41 residues. Each  $\alpha$ - and  $\beta$ -subunit binds three BChl *a* cofactors.<sup>3</sup> One of the BChls connected to the  $\alpha$ -subunit participates in a ring of nine BChls, which shows an absorption maximum at 800 nm that corresponds with an absorption energy of  $12\,500\text{ cm}^{-1}$ . The remaining two BChls, one connected to the  $\alpha$ -subunit and one connected to the  $\beta$ -subunit, participate in a concentric ring of

<sup>†</sup> Leiden University.

<sup>‡</sup> University of Glasgow.

(1) Cogdell, R. J.; Isaacs, N. W.; Freer, A. A.; Arrelano, J.; Howard, T. D.; Papiz, M. Z.; Hawthornthwaite-Lawless, A. M.; Prince, S. *Prog. Biophys. Mol. Biol.* **1997**, *68*, 1–27.  
(2) Hoff, A. J.; Deisenhofer, J. *Phys. Rep.* **1997**, *287*, 2–247.

(3) Papiz, M. Z.; Prince, S. M.; Howard, T.; Cogdell, R. J.; Isaacs, N. W. *J. Mol. Biol.* **2003**, *326*, 1523–1538.

(4) Koepke, J.; Hu, X. C.; Muenke, C.; Schulten, K.; Michel, H. *Structure* **1996**, *4*, 581–597.

18 BChls, which has an absorption maximum at 860 nm corresponding to an absorption energy of  $11\,627\text{ cm}^{-1}$ . Throughout the paper, we refer to these cofactors as the B800,  $\alpha\text{B}850$ , and  $\beta\text{B}850$  cofactors. The  $\alpha\text{B}850$  and  $\beta\text{B}850$  in every monomeric unit form a pair of partly overlapping BChls that is sandwiched between the  $\alpha$ - and  $\beta$ -subunits. Each pair also overlaps with the pair of the adjacent monomeric unit, forming a ring with continuous overlap between the 18 B850 cofactors. The nine B800 cofactors are positioned between the transmembrane helices of the  $\beta$ -subunits of each LH2 unit and form a ring without mutual overlap. The maximum absorption wavelengths of the B800 and B850 in the LH2 complex from *Rps. acidophila* are the  $Q_y$ -absorption bands. This refers to the  $Q_y$  dipole moment of the BChls, which can be physically mapped in the plane surface on the long axis of the  $\pi$ -bonding system in the ring system of the cofactors. The  $Q_y$ -bands of the B800 and the B850 in the LH2 complex differ substantially from the spectrum of monomeric BChl *a* complexes in acetone: methanol 7:3 solution at 773 nm, corresponding with an energy of  $12937\text{ cm}^{-1}$ .<sup>5</sup> The  $Q_y$  bands are 30 and 85 nm red shifted, respectively. It is known that protein–cofactor interactions and cofactor–cofactor interactions in the LH2 both contribute to the shift of the  $Q_y$  absorption band.<sup>6</sup> In addition to the pronounced shift of the  $Q_y$  band, there is a small shift of the  $Q_x$  band, which is primarily due to coordination effects.<sup>7</sup>

MAS NMR spectroscopy is able to specify the ground-state electronic structure of the BChls in the photoactive complexes. For instance, recently MAS NMR and photo-CIDNP were combined and performed on photosynthetic reaction centers of *Rb. sphaeroides*, containing biosynthetic specifically  $^{13}\text{C}$ -enriched BChls in the special pair, and it was found that the electronic structure of the BChls in the reaction center is asymmetric.<sup>8</sup> Recently, MAS NMR has also been used for a chemical shift assignment of the partly and fully labeled reconstituted retinylidene chromophore in rhodopsin and has revealed the electronic structure in the ground state of the native form.<sup>9,10</sup> Here, we use MAS dipolar correlation NMR spectroscopy to selectively assign the responses of BChls in the uniformly labeled LH2 protein complex isolated from *Rps. acidophila* strain 10050 and resolve how the cofactor–cofactor interactions and the protein environment tune the electronic structures of these cofactors. We resolve the electronic differences for B800 and B850 in their natural environment by comparing the solid-state isotropic  $^{13}\text{C}$  chemical shifts ( $\sigma_{\text{B}800}^{\text{S}}$ ,  $\sigma_{\text{B}850}^{\text{S}}$ ) with the shifts for monomeric BChls dissolved in acetone- $d_6$  ( $\sigma^{\text{L}}$ ). Density functional theory (DFT) calculations were performed to estimate the ring current effects for the B850. After correction for the ring current shifts, the molecular electronic ground state of the B850 could be characterized with atomic selectivity, and global interactions with the LH2 protein matrix are resolved.

## Materials and Methods

Uniformly [ $^{13}\text{C}$ , $^{15}\text{N}$ ]-enriched LH2 complexes were obtained by growing *Rps. acidophila* strain 10050 anaerobically in light at 30 °C on a defined medium.<sup>11</sup> The amounts of [U- $^{13}\text{C}$ , $^{15}\text{N}$ ]-labeled algae hydrolysate (Cambridge Isotopes Laboratories, Andover, MA) and  $^{13}\text{C}_4$ -labeled succinic acid were adjusted to 1.5 and 2.0 g/L, respectively, to optimize the cell growth. The  $^{13}\text{C}_4$ -enriched succinic acid was prepared by a multistep synthesis, starting with the synthesis of fumaric acid from  $^{13}\text{C}_2$ -labeled acetic acid (CIL, Andover, MA).<sup>12</sup> In the final step, fumaric acid was converted to succinic acid in a reduction reaction with  $\text{H}_2$  and Pd–C as catalyst. After growing for 8 days, cells were harvested, and the LH2 complexes were isolated.<sup>13</sup> The sample was concentrated to a volume of  $\sim 0.10$  mL using a Centricon 100-kDa filter. The concentrated sample was transferred into a 4.0-mm CRAMPS rotor, containing approximately 10 mg of protein. The U-[ $^{13}\text{C}$ , $^{15}\text{N}$ ]-B800 LH2 complex was prepared by selective removal of the B800 molecule from the unlabeled LH2 complex, where the B800 binding site was reconstituted with U-[ $^{13}\text{C}$ , $^{15}\text{N}$ ]-BChl *a*, using the reconstitution method described elsewhere.<sup>14</sup>

Radio frequency-driven dipolar recoupling (RFDR) and proton-driven spin diffusion (PDS) techniques were used to record  $^{13}\text{C}$ – $^{13}\text{C}$  correlation data with a Bruker AV-750 spectrometer using a double channel CP-MAS probe head. The proton  $\pi/2$  pulse was set to 3.1  $\mu\text{s}$ , corresponding to a nutation frequency of 80.6 kHz, while a  $^{13}\text{C}$  B<sub>1</sub> field strength of 50 kHz with a cross polarization time of 2.0 ms was used during a 100–50% ramped CP sequence.<sup>15</sup> 2D  $^{13}\text{C}$ – $^{13}\text{C}$  RFDR spectra were acquired at a radio frequency of 188.6 MHz by using a pathway-selective phase cycling method.<sup>16</sup> The protons were decoupled by use of continuous wave (CW) decoupling of 80.6 kHz during the mixing time and by two-pulse phase modulation (TPPM) decoupling during  $t_1$  and  $t_2$ .<sup>17</sup> Rotor-synchronized  $\pi$ -pulses with a length of 8.4  $\mu\text{s}$  were applied during the mixing time. For optimal signal intensity in the aromatic region, the carrier frequency was set at 130 ppm on the chemical shift scale. For the PDS NMR experiment, the proton decoupling was switched off during the spin diffusion mixing period to obtain  $^1\text{H}$ -mediated transfer of  $^{13}\text{C}$  polarization along the molecular carbon network.

Samples were cooled to 223 K to immobilize the sample while maintaining good spectral resolution, and the MAS spinning frequency  $\omega_{\text{R}}/2\pi$  was 13 kHz. Additional PDS and RFDR NMR spectra were collected with spinning frequencies of 10.2 kHz to resolve correlations located at the spinning sidebands. Mixing times of 2.5 ms (RFDR) and 15 ms (PDS) were long enough to observe the correlations between directly bonded carbons as well as relayed correlations between more remote positions. To resolve all resonances, both 2D RFDR and PDS  $^{13}\text{C}$ – $^{13}\text{C}$  correlation NMR spectra of the U-[ $^{13}\text{C}$ , $^{15}\text{N}$ ] LH2 and the U-[ $^{13}\text{C}$ , $^{15}\text{N}$ ]-B800 LH2 were recorded. The  $^{13}\text{COOH}$  resonance of U-[ $^{13}\text{C}$ , $^{15}\text{N}$ ]-tyrosine·HCl at 172.1 ppm was used as an external chemical shift reference to determine the isotropic chemical shifts ( $\sigma$ ) of the B800/B850 carbons.

To calculate the local magnetic shielding due to the local magnetic field induced by the ring current effect in the BChls ( $\sigma^{\text{R}}$ ), the nucleus-independent chemical shift (NICS) calculation with the DFT method

- (5) Scheer, H. In *The Chlorophylls*; Scheer, H., Ed.; CRC: Boca Raton, FL, 1991.
- (6) Cogdell, R. J.; Howard, T. D.; Isaacs, N. W.; McLuskey, K.; Gardiner, A. T. *Photosynth. Res.* **2002**, *74*, 135–141.
- (7) Evans, T. A.; Katz, J. J. *Biochim. Biophys. Acta* **1975**, *396*.
- (8) Schulten, E. A. M.; Matsysik, J.; Alia; Kiihne, S.; Raap, J.; Lugtenburg, J.; Gast, P.; Hoff, A. J.; de Groot, H. J. M. *Biochemistry* **2002**, *41*, 8708–8717.
- (9) Verhoeven, M. A.; Creemers, A. F. L.; Bovee-Geurts, P. H. M.; De Grip, W. J.; Lugtenburg, J.; de Groot, H. J. M. *Biochemistry* **2001**, *40*, 3282–3288.
- (10) Creemers, A. F. L.; Kiihne, S.; Bovee-Geurts, P. H. M.; DeGrip, W. J.; Lugtenburg, J.; de Groot, H. J. M. *Proc. Natl. Acad. Sci. U.S.A.* **2002**, *99*, 9101–9106.

- (11) Egorova-Zachernyuk, T. A.; Hollander, J.; Fraser, N.; Gast, P.; Hoff, A. J.; Cogdell, R.; de Groot, H. J. M.; Baldus, M. *J. Biomol. NMR* **2001**, *19*, 243–253.
- (12) Heinen, W. *Grafting of polyolefins and miscibility in copolymer mixtures*; Leiden University: Leiden, 1996.
- (13) Hawthorthwaite-Lawless, A. M.; Cogdell, R. J. In *The Chlorophylls*; Scheer, H., Ed.; CRC: Boca Raton, FL, 1991; pp 494–528.
- (14) Fraser, N. J.; Dominy, P. J.; Ucker, B.; Simonin, I.; Scheer, H.; Cogdell, R. J. *Biochemistry* **1999**, *38*, 9684–9692.
- (15) Metz, G.; Wu, X. L.; Smith, S. O. *J. Magn. Reson., Ser. A* **1994**, *110*, 219–227.
- (16) Boender, G. J.; Vega, S.; de Groot, H. J. M. *J. Chem. Phys.* **2000**, *112*, 1096–1106.
- (17) Bennett, A. E.; Rienstra, C. M.; Griffiths, J. M.; Zhen, W. G.; Lansbury, P. T.; Griffin, R. G. *J. Chem. Phys.* **1998**, *108*, 9463–9479.

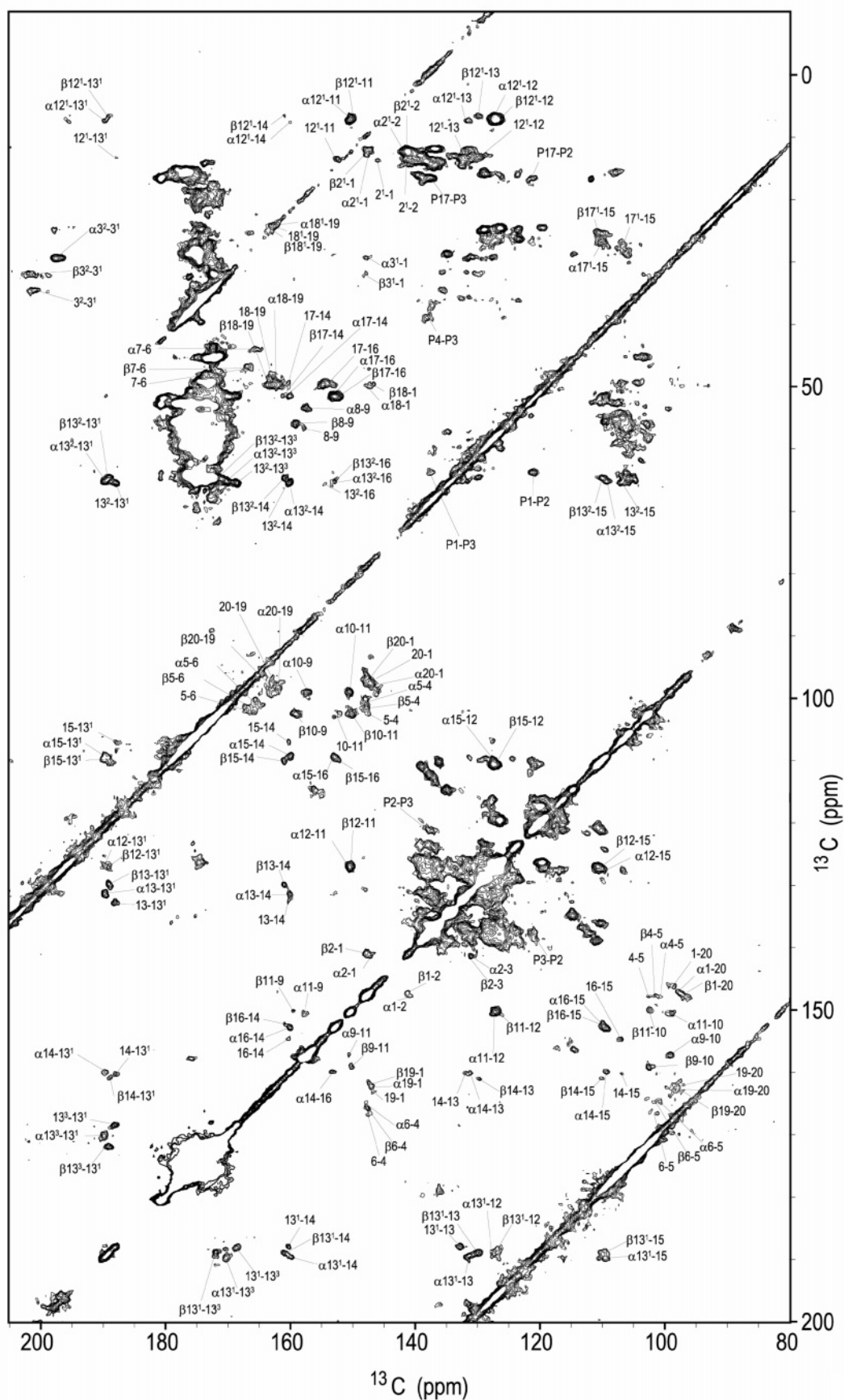


**Figure 1.** Contour plot of a high-resolution MAS 2D  $^{13}\text{C}$ – $^{13}\text{C}$  RFDR solid-state NMR spectrum of the  $[U\text{-}^{13}\text{C}, ^{15}\text{N}]$  LH2 complex isolated from *Rps. acidophila* strain 10050. The data were obtained at 223 K with a spinning frequency of 13 kHz and a RFDR mixing time of 2.5 ms. The chemical shift correlation networks of the B800, the  $\alpha$ B850, and the  $\beta$ B850 are indicated using the IUPAC numbering shown in Figure 2.  $\alpha$ B850 and  $\beta$ B850 are indicated by  $\alpha$  and  $\beta$ , respectively.



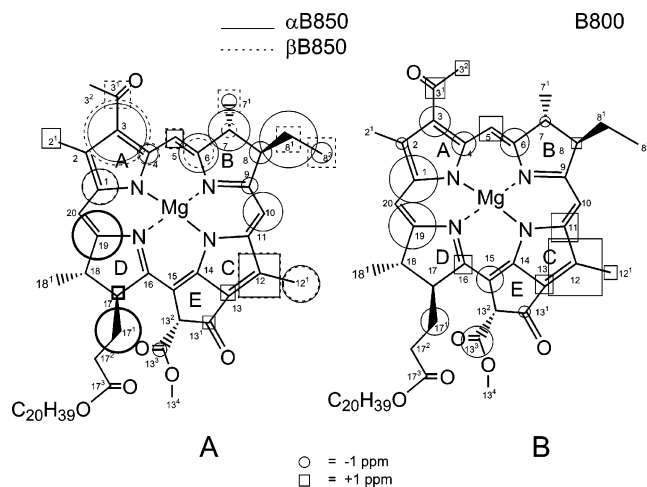


**Figure 2.** Estimated electronic shift changes ( $|\Delta\delta| \geq 1.0$  ppm), represented by circles (shielding effects) and squares (deshielding effects) for the  $\alpha$ B850 and  $\beta$ B850 (A) and the B800 (B) cofactors in the LH2 complex. The size of the mark is proportional to the magnitude of  $\Delta\delta$ .

based on Becke's<sup>18</sup> and Lee–Young–Parr's<sup>19</sup> gradient-corrected correlation functional (BLYP) was used. Calculations were performed at the BLYP/6-31G(d,p) level using the GIAO method as implemented in the Gaussian 98 package.<sup>20</sup> The geometries of the B850 cofactors were taken directly from the X-ray coordinates without any further geometry relaxation. To simplify the calculations, the phytol tail connected to C17 was substituted by a methyl group. The  $\sigma_{\text{B850}}^{\text{R}}$  were calculated for each carbon, which is in the shielding area of an adjacent overlapping B850. The coordinates of the carbons affected by the ring current were used as points in space, and the shielding effect induced by the adjacent B850 was calculated at these positions. Four calculations were performed: two for the overlap between rings A, and two for the overlap between rings C (Figure 2). The macrocycle of  $\alpha$ B850 was used to calculate the shielding on carbons from the interacting  $\beta$ B850. In a next calculation, the macrocycle of the  $\beta$ B850 was used to calculate the shielding on carbons from the interacting  $\alpha$ B850. This leads to independent calculations of the ring current effect without contributions from the  $\pi$ – $\pi$  overlap and other electronic effects.

Electronic changes in B800 and B850 cofactors induced by the molecular environment were identified by measuring isotropic  $^{13}\text{C}$  chemical shift differences ( $\Delta\sigma$ ) between monomeric BChl *a* and B800/B850, defined as  $\Delta\sigma = \sigma^{\text{S}} - \sigma^{\text{I}}$ . For B800, the  $\Delta\sigma_{\text{B800}}$  represents an estimate of the shift changes due to the cofactor–protein interactions. The mutual distances between the B800 are too large to induce significant ring current effects.<sup>21</sup> The  $\Delta\sigma_{\text{B850}}$  for carbons in the B850 are corrected for the ring current contribution to the chemical shift  $\sigma^{\text{R}}$  from the adjacent B850. This yields an estimate of the chemical shift change  $\Delta\delta_{\text{B850}}$  due to the interactions with the protein matrix, according to

$$\Delta\delta_{\text{B850}} = \Delta\sigma_{\text{B850}} - \sigma_{\text{B850}}^{\text{R}} \quad (1)$$

(18) Becke, A. D. *J. Chem. Phys.* **1986**, *84*, 4524.

(19) Lee, C. T.; Yang, W. T.; Parr, R. G. *Phys. Rev. B* **1988**, *37*, 785–789.

(20) Frisch, M. J.; Trucks, G. W.; Schlegel, H. B.; Scuseria, G. E.; Robb, M. A.; Cheeseman, J. R.; Zakrzewski, V. G.; Montgomery, J. A., Jr.; Stratmann, R. E.; Burant, J. C.; Dapprich, S.; Millam, J. M.; Daniels, A. D.; Kudin, K. N.; Strain, M. C.; Farkas, O.; Tomasi, J.; Barone, V.; Cossi, M.; Cammi, R.; Mennucci, B.; Pomelli, C.; Adamo, C.; Clifford, S.; Ochterski, J.; Petersson, G. A.; Ayala, P. Y.; Cui, Q.; Morokuma, K.; Malick, D. K.; Rabuck, A. D.; Raghavachari, K.; Foresman, J. B.; Cioslowski, J.; Ortiz, J. V.; Stefanov, J. B.; Liu, G.; Liashenko, A.; Piskorz, P.; Komaromi, I.; Gomperts, R.; Martin, R. L.; Fox, D. J.; Keith, T.; Al-Laham, M. A.; Peng, C. Y.; Nanayakkara, A.; Gonzalez, C.; Challacombe, M.; Gill, P. M. W.; Johnson, B.; Chen, W.; Wong, M. W.; Andres, J. L.; Gonzalez, C.; Head-Gordon, M.; Replogle, E. S.; Pople, J. A. *Gaussian 98*, revision A.5; Gaussian, Inc.: Pittsburgh, PA, 1998.

## Results

The high-resolution 2D RFDR  $^{13}\text{C}$ – $^{13}\text{C}$  NMR spectrum of the U- $^{13}\text{C}$ ,  $^{15}\text{N}$  LH2 complex, shown in Figure 1, can be subdivided into two parts. In the upper part of the figure, between 0 and 75 ppm, the correlations from the aliphatic protein response of the U- $^{13}\text{C}$ ,  $^{15}\text{N}$  LH2 complex are observed. The lower part, between 100 and 200 ppm, shows the correlation signals involving aromatic moieties. Most correlation signals from the BChl *a* cofactors in the LH2 complex can be resolved from the spinning sidebands by using a spinning frequency of 13 kHz. The various  $^{13}\text{C}$  correlation signals for the aromatic  $^{13}\text{C}$  carbons from the BChl *a* cofactors are labeled with a number that corresponds to the carbon positions in the macrocycle according to the IUPAC numbering shown in Figure 2.

Aromatic carbons can be assigned from their nearest-neighbor correlations. In Figure 1, the C3–C3<sup>1</sup> correlations coincide with the spinning sidebands, and they can be resolved in a dataset recorded with a spinning frequency of 10.2 kHz. The aliphatic C2<sup>1</sup>, C7, C8, C12, C13<sup>2</sup>, C17, and C18 can be assigned via correlations with adjacent aromatic carbons. In addition, the aliphatic carbons C7<sup>1</sup>, C8<sup>1</sup>, C8<sup>2</sup>, C17<sup>1</sup>, C17<sup>2</sup>, and C18<sup>1</sup> are assigned from the long-range correlations to aromatic carbons. C18<sup>1</sup> and C17<sup>1</sup> are observed weakly in the upper part of the RFDR NMR spectrum, while correlations between C7<sup>1</sup>, C8<sup>1</sup>, C8<sup>2</sup>, and C17<sup>1</sup> could be assigned from the crowded aliphatic region contour region in the PDS NMR spectrum (data not shown). Due to the relatively high local density of  $^1\text{H}$  nuclei, which mediate the magnetization transfer in the PDS technique, strong correlation signals of the aliphatic carbons are observed in the PDS NMR spectrum that complement the RFDR dataset.

Finally, there is strong overlap between the C17<sup>2</sup>–C17<sup>3</sup> correlation signals and the broad correlation response from the carbonyl carbons between  $\sim 170$  and  $\sim 180$  ppm with the aliphatic C $\alpha$  and C $\beta$  carbons between 0 and 75 ppm. This makes an assignment of the C17<sup>3</sup> difficult. In contrast, the cofactor signals involving the C3<sup>1</sup>, C13<sup>1</sup>, and C13<sup>3</sup> have a good dispersion and are also well resolved by the long-range correlations due to the relayed transfer along the  $^{13}\text{C}$  molecular framework.

For each BChl *a* cofactor species, a distinct network of nearest-neighbor carbon correlations can be identified by analyzing the correlations of the ring A carbons with carbons further in the molecular network by relayed transfer. With the help of another dataset collected from the  $^{13}\text{C}$ ,  $^{15}\text{N}$ –B800 LH2 sample, the correlation network from the B800 can be assigned unambiguously. The two remaining datasets belong to the B850. The shift assignments are summarized in Table 1.

The  $\sigma^{\text{R}}$  calculated with DFT for nuclei in the pyrrole rings A and C of the B850 cofactors are summarized in Table 1. The  $\sigma^{\text{R}}$  are largest for C2, C2<sup>1</sup>, C3, C3<sup>1</sup>, and C3<sup>2</sup> from ring A and for positions C12, C12<sup>1</sup>, C13, and C13<sup>1</sup> from ring C. The pyrrole rings A and C are within 3.9 and 3.6 Å of the macrocycle of an adjacent cofactor, respectively, and experience the largest local magnetic field effects induced by the ring current.<sup>3</sup> A large difference between  $\sigma_{\alpha\text{B850}}^{\text{R}}$  and  $\sigma_{\beta\text{B850}}^{\text{R}}$  was calculated for carbons C2, C2<sup>1</sup>, C3, C3<sup>1</sup>, and C3<sup>2</sup> from ring A. The chemical shift differences between the  $\alpha$ B850 and  $\beta$ B850 are small. The

(21) Freer, A.; Prince, S.; Sauer, K.; Papiz, M.; Hawthornthwaite-Lawless, A.; McDermott, G.; Cogdell, R.; Isaacs, N. W. *Structure* **1996**, *4*, 449–462.

**Table 1.** Summary of the Isotropic Chemical Shift ( $\sigma$ ), the Isotropic Chemical Shift of BChl *a* Monomers in Acetone ( $\sigma^A$ ), the Isotropic Chemical Shift Difference between Monomeric BChl in Acetone and Cofactors in the LH2 Complex ( $\Delta\sigma$ ), the Ring Current Shift Calculated with DFT ( $\sigma^R$ ), and the Chemical Shift Change Due to Electronic Effects ( $\Delta\tilde{\sigma}$ )

carbon	$\sigma_{B800}$	$\sigma_{\alpha B850}$	$\sigma_{\beta B850}$	$\sigma^I$	$\Delta\sigma_{B800}$	$\Delta\sigma_{\alpha B850}$	$\Delta\sigma_{\beta B850}$	$\sigma_{B850}^R(\alpha,\beta)$	$\Delta\tilde{\sigma}_{\alpha B850}$	$\Delta\tilde{\sigma}_{\beta B850}$
1	146.2	147.1	147.8	151.2	-5.0	-4.1	-3.4	-0.75, -0.14	-3.4	-3.3
2	141.0	141.1	141.3	142.1	-1.1	-1.0	-0.8	-1.93, -0.86	0.9	0.1
2 <sup>1</sup>	13.3	12.3	12.2	13.5	-0.2	-1.2	-1.3	-3.10, -1.41	1.9	0.1
3	134.4	130.3	130.7	137.6	-3.2	-7.3	-6.9	-1.71, -0.74	-5.6	-6.2
3 <sup>1</sup>	201.4	197.9	201.1	199.3	2.1	-1.4	1.8	-1.72, -0.72	0.3	2.5
3 <sup>2</sup>	34.4	29.2	31.9	32.9	1.5	-3.7	-1.0	-2.81, -1.32	-0.9	0.3
4	147.7	147.7	147.9	150.2	-2.5	-2.5	-2.3	-0.70, -0.19	-1.8	-2.1
5	102.1	100.8	101.5	99.6	2.5	1.2	1.9	-0.40, -0.14	1.6	1.8
6	165.9	165.2	166.1	168.9	-3.0	-3.7	-2.8		-3.7	-2.8
7	47.2	44.3	46.8	48.2	-1.0	-3.9	-1.4		-3.9	-1.4
7 <sup>1</sup>	a	22.1	25.3	23.1		-1.0	2.2		-1.0	2.2
8	56.6	53.5	56.1	55.6	1.0	-2.1	0.5		-2.1	0.5
8 <sup>1</sup>	a	25.4	32.3	30.8		-5.4	2.3		-5.4	2.3
8 <sup>2</sup>	a	9.1	13.2	10.5		-1.4	2.7		-1.4	2.7
9	157.8	157.4	159.2	158.5	-0.7	-1.1	0.7		-1.1	0.7
10	102.6	99.0	102.5	102.4	0.2	-3.4	0.1	0.27, 0.05	-3.7	0.1
11	152.4	150.5	150.1	149.5	2.9	1.0	0.6	0.10, -0.21	0.9	0.8
12	129.7	127.3	126.9	123.9	5.8	3.4	3.0	-0.56, -1.05	4.0	4.1
12 <sup>1</sup>	13.3	7.2	6.6	11.9	1.4	-4.7	-5.3	-1.25, -2.04	-3.5	-3.3
13	132.4	131.4	129.9	130.5	1.9	0.9	-0.6	-0.50, -0.78	1.4	0.2
13 <sup>1</sup>	187.9	189.7	189.1	189.0	-1.1	0.7	0.1	-0.46, -0.55	1.2	0.7
13 <sup>2</sup>	65.3	65.2	64.7	65.7	-0.4	-0.5	-1.0	-0.06, -0.09	-0.4	-0.9
13 <sup>3</sup>	168.3	170.3	172.0	171.6	-3.3	-1.3	0.4		-1.3	0.4
14	160.1	160.0	161.0	160.8	-0.7	-0.8	0.2	-0.02, -0.22	-0.8	0.4
15	106.9	109.4	110.1	109.7	-2.8	-0.3	0.4	0.03, -0.07	-0.3	0.4
16	154.1	153.1	152.3	152.2	1.9	0.9	0.1		0.9	0.1
17	49.7	51.6, 51.7		50.5	-0.8	1.1, 1.2				
17 <sup>1</sup>	27.6	26.8, 26.3		30.5	-2.9	-3.7, -4.2				
17 <sup>2</sup>	a	a		29.4						
17 <sup>3</sup>	a	a		173.4						
18	49.1	49.8, 49.6		49.3	-0.2	0.5, 0.3				
18 <sup>1</sup>	24.2	24.2, 24.2		23.3	0.9	0.9, 0.9				
19	162.4	162.3, 162.7		167.3	-4.9	-5.0, -4.6				
20	96.9	97.2, 97.6		96.3	0.6	0.9, 1.3				

<sup>a</sup> Correlation peaks are not observed.

DFT calculations on the B850 cofactors indicate that the  $\alpha$ B850 experiences a stronger shielding effect than the  $\beta$ B850. Hence, the shift correlation set that is most shielded has been assigned to the  $\alpha$ B850, while the other set is attributed to the  $\beta$ B850. Outside the overlap region, the responses of the  $\alpha$ B850 and  $\beta$ B850 are very similar, which shows that the electronic differences between  $\alpha$ B850 and  $\beta$ B850 cofactors are small.

The shifts associated with electronic changes in the B800 relative to the monomeric BChl *a* in solution ( $\Delta\sigma_{B800}$ ) can be directly determined from the observed  $\Delta\sigma_{B800}$ . The mutual distance of 21.2 Å between B800 cofactors is too large to exert a significant shielding effect on nearby B800 cofactors.<sup>21</sup> After the corrections for the ring current were applied according to eq 1, the shift differences between the B800,  $\alpha$ B850, and  $\beta$ B850 are minimal. The  $\Delta\tilde{\sigma}_{B850}$  of the <sup>13</sup>C in the bacteriochlorin ring are summarized in Table 1, while the  $\Delta\tilde{\sigma}_{B850}$  with  $|\Delta\tilde{\sigma}_{B850}| \geq 1.0$  ppm are represented by proportional squares and circles in Figure 2A. The solid and dashed lines in the figure represent the electronic effects on the  $\alpha$ B850 and  $\beta$ B850, respectively. C17, C17<sup>1</sup>, and C19 were not specifically assigned to  $\alpha$ B850 or  $\beta$ B850. For these positions, the  $\Delta\tilde{\sigma}_{B850}$  are of the same order for the  $\alpha$ B850 and the  $\beta$ B850 and are indicated in Figure 2A with thick solid contours.

## Discussion

The changes of the chemical shifts with respect to monomeric BChl *a* in acetone-*d*<sub>6</sub> can be used to assess the electronic perturbations in the cofactors, which contribute to the red-shifted

Q<sub>y</sub> bands of the B800 and the B850 cofactors in their natural environment. In general, from the  $\Delta\tilde{\sigma}_{B850}$  represented in Figure 2A and B, it is evident that the electronic polarization effects in all three cofactor species are of the same order. The differences could arise from various mechanisms, such as structural differences or different protein-cofactor interactions. X-ray data show that the  $\beta$ B850 is bent, while  $\alpha$ B850 is planar. This may explain why minor shift differences between the two species in the NMR correlation spectrum are observed. The NMR spectra show that this structural difference provokes very small electronic differences between the ground states of the two B850 species. This contrasts with recent model studies by Fajer et al. and Senger et al.<sup>22,23</sup> Their studies demonstrated that, in principle, structural distortions can have a pronounced effect on the electronic structure, although the distortions for their molecules were much larger than for the B850 macrocycles in the LH2 complex.

The strongest negative  $\Delta\tilde{\sigma}$  are detected for the  $\pi$ -carbons located in and close to ring A, while pronounced positive  $\Delta\tilde{\sigma}$  are detected for carbons in ring C. The negative  $\Delta\tilde{\sigma}$  are distributed over aromatic carbons located between C6 and C19 around ring A, while the positive  $\Delta\tilde{\sigma}$  distribution is restricted to predominantly C11, C12, and C13 in ring C. The chemical shift changes indicate a stabilization of partly negative charge density ( $\delta^-$ ) at and around ring A and polarized positive charge

(22) Fajer, J. J. *Porphyryns Phthalocyanines* 2000, 4, 382–385.

(23) Senger, M. O.; Renner, M. W.; Kalisch, W. W.; Fajer, J. J. *Chem. Soc., Dalton Trans.* 2000, 381–385.

( $\delta^+$ ) at ring C, corresponding with an induced electronic dipole moment parallel to the long axis of the  $\pi$ -bonding system and to the  $Q_y$  transition dipole moment. The difference between the negative-induced charge at the vicinity of ring A and the positive-induced charge at ring C induces approximately  $\sim 20$ – $25$  ppm cumulative shift effects for both cofactors species, representing comparable dipole strengths along the long axis of the bacteriochlorin ring in the ground states. The dipole of the  $\alpha$ B850 is slightly different as compared to the others, due to the relative large negative  $\Delta\tilde{\sigma}$  observed at C9 and C10.

The electronic effects are distributed over a relatively large part of the molecular structure of the B800 and B850 macrocycles. This implies that local interactions, like the hydrogen-bond interaction of the C3-acetyl group and the axial coordination of the Mg, cannot explain the color shifts in the LH2. The NMR data provide evidence for global mutual polarization effects between the cofactors and their protein environment. In this picture, the polarity of the environment affects the dielectric properties of the LH2 protein interior, leading to a collective effect on the B800 and B850 electronic structure. Local interactions can still be essential structural elements provoking changes of the protein functional characteristics upon removal of the hydrogen-bonding groups as shown by mutation studies.<sup>24–29</sup> A clear example is provided for the B800/B820 or LH3 complex, which is a spectroscopic variant of the LH2.<sup>29</sup> In the active binding site of the cofactors of this complex, a specific amino acid holds the C3-acetyl groups in an out-of-plane orientation, thereby changing the properties of the cofactors. DFT calculations performed on  $\alpha$ B850 indicate a significant blue shift for the BChls with the C3-acetyl group perpendicular to the plane of the macrocycle with regard to the C3-acetyl in a coplanar orientation. This is in line with previous theoretical calculations.<sup>30</sup>

Mutation studies on the protein environment that surrounds the cofactors of the reaction center in *Rb. sphaeroides* have shown that the dielectrics of environment of the cofactors is affected by charge separation in a nonlinear response mechanism due to synergistic contributions of various chemical functional polar groups, leading to changes of the absorption wavelengths of the cofactors.<sup>31</sup> This has been confirmed by chemical modeling, which includes the dielectrics of the protein environment of the photosynthetic reaction center.<sup>32</sup>

The narrow NMR signals of the bacteriochlorin ring carbons in the 2D RFDR NMR spectrum show that the LH2 complexes in the sample are well ordered and all LH2 units of the nonameric aggregate complex are from the NMR point of view spectroscopically identical. When viewed on a fast time-scale in the excited state, disorder can be observed, as has been

demonstrated by time-resolved optical studies.<sup>33–36</sup> The NMR study shows narrow resonances. This shows that the ground-state structure on the much longer NMR time-scale is on average very regular, in line with X-ray studies. If there are differences between the site energies of the individual BChl, the effect on the electronic structure should be small as compared to the difference between the  $\alpha$ -B850 and  $\beta$ -B850, which is clearly resolved in the NMR spectra. Of the long phytol chains, only the p1, p2, p3, and p17 carbons are detected, which suggests that the tails may be disordered in the frozen sample.

Because the  $Q_y$  band of B800 has a red shift of  $\sim 30$  nm ( $437$   $\text{cm}^{-1}$ ) and the induced electronic effects and corresponding electronic dipoles in the B800 and B850 are similar, it is difficult to attribute the additional red shift of  $60$  nm ( $873$   $\text{cm}^{-1}$ ) for the B850 cofactors to electronic changes of the ground state. Structure-based calculations performed on LH2 that use a point monopole approximation to represent B800 and B850  $Q_y$  dipole transition moments indicate that the coupling between the 18 B850 rings in LH2 yields a  $40$  nm red shift as compared to the  $Q_y$  band of the ring of nine B800 cofactors, assuming that the site energies are identical for both cofactor species.<sup>37</sup> This corresponds to a  $Q_y$  band at  $840$  nm for the B850 cofactors. When the  $\Delta\tilde{\sigma}$  on the B800 are associated to the  $\sim 30$  nm red shift from monomeric BChl *a* in solution to the protein environment, it is virtually impossible that the small  $\Delta\tilde{\sigma}$  differences between the B800 and B850 represent the B800–B850 absorption difference. Hence, the large B800–B850 absorption difference should be attributed predominantly to excitonic coupling between the transition dipole moments of the B850 cofactors.<sup>35,36</sup>

In addition to the changes of the electric dipole moment of the rings, the cumulative  $\Delta\tilde{\sigma} < 0$  imply a negative charge on the bacteriochlorin rings. This is in line with recent studies that have shown that the imidazole moieties of the Mg-coordinating histidines in the LH2 protein are positively charged, because the positive charge at the imidazole is compensated and stabilized by negative charge at the BChl.<sup>38,39</sup> The cumulative  $\Delta\tilde{\sigma}$  are  $-8.1$ ,  $-14.4$ , and  $-9.4$  ppm for B800,  $\alpha$ B850, and  $\beta$ B850, respectively. A detailed analysis of the electronic effects shows that the balances between the positive- and negative-induced charge effects in B800 and B850 are slightly different. Comparing the positive  $\Delta\tilde{\sigma}$  effects in the vicinity of ring C clearly suggests that this area in the B800 is more positively charged than the corresponding area of the  $\alpha$ B850 and  $\beta$ B850. The cumulative  $\Delta\tilde{\sigma} < 0$  effects on the aromatic carbons in the vicinity of ring A are similar for all three cofactor species. Pronounced  $\Delta\tilde{\sigma}$  differences between the negative  $\Delta\tilde{\sigma}$  distributions in the B800 and B850 cofactors are observed at C1 and C3. In the B800 complexes, a strong  $\Delta\tilde{\sigma}$  effect is observed for C1 and a moderate  $\Delta\tilde{\sigma}$  effect is detected for C3, while the

- (24) Fowler, G. J. S.; Visschers, R. W.; Grief, G. G.; Vangrondelle, R.; Hunter, C. N. *Nature* **1992**, *355*, 848–850.  
 (25) Fowler, G. J. S.; Sockalingum, G. D.; Robert, B.; Hunter, C. N. *Biochem. J.* **1994**, *299*, 695–700.  
 (26) Fowler, G. J. S.; Hess, S.; Pullerits, T.; Sundstrom, V.; Hunter, C. N. *Biochemistry* **1997**, *36*, 11282–11291.  
 (27) Gall, A.; Ridge, J. P.; Robert, B.; Cogdell, R. J.; Jones, M. R.; Fyfe, P. K. *Photosynth. Res.* **1999**, *59*, 223–230.  
 (28) Gall, A.; Fowler, G. J. S.; Hunter, C. N.; Robert, B. *Biochemistry* **1997**, *36*, 16282–16287.  
 (29) McLuskey, K.; Prince, S. M.; Cogdell, R. J.; Isaacs, N. W. *Biochemistry* **2001**, *40*, 8783–8789.  
 (30) Gudowska-Nowak, E.; Newton, M. D.; Fajer, J. *J. Phys. Chem.* **1990**, *94*, 5795–5801.  
 (31) Moore, L. J.; Zhou, H. L.; Boxer, S. G. *Biochemistry* **1999**, *38*, 11949–11960.  
 (32) Sham, Y. Y.; Muegge, I.; Warshel, N. *Biophys. J.* **1999**, *76*, A198–A198.

- (33) van Oijen, A. M.; Ketelaars, M.; Matsushita, M.; Kohler, J.; Aartsma, T. J.; Schmidt, J. *Biophys. J.* **2001**, *80*, 151A–151A.  
 (34) van Oijen, A. M.; Ketelaars, M.; Kohler, J.; Aartsma, T. J.; Schmidt, J. *Chem. Phys.* **1999**, *247*, 53–60.  
 (35) van Oijen, A. M.; Ketelaars, M.; Kohler, J.; Aartsma, T. J.; Schmidt, J. *Science* **1999**, *285*, 400–402.  
 (36) Georgakopoulou, S.; Frese, R. N.; Johnson, E.; Koolhaas, C.; Cogdell, R. J.; van Grondelle, R.; van der Zwan, G. *Biophys. J.* **2002**, *82*, 2184–2197.  
 (37) Sauer, K.; Cogdell, R. J.; Prince, S. M.; Freer, A.; Isaacs, N. W.; Scheer, H. *Photochem. Photobiol.* **1996**, *64*, 564–576.  
 (38) van Gammeren, A. J.; Hulsbergen, F. B.; Erkelens, C.; de Groot, H. J. M. *J. Biol. Inorg. Chem.* **2004**, *9*, 109–117.  
 (39) Alia; Matysik, J.; Soede-Huijbrechts, C.; Baldus, M.; Raap, J.; Lugtenburg, J.; Gast, P.; van Gorkom, H. J.; Hoff, A. J.; de Groot, H. J. M. *J. Am. Chem. Soc.* **2001**, *123*, 4803–4809.

reverse effect for those carbons is observed in the B850. The C3-acetyl groups of the B850 are twisted as compared to the C3-acetyl group of B800 and may contribute to the chemical shift differences.

Finally, shift differences are observed for C7, C7<sup>1</sup>, C8, C8<sup>1</sup>, C8<sup>2</sup>, C13<sup>1</sup>, C17, and C17<sup>1</sup> of  $\alpha$ B850 and  $\beta$ B850. It is believed that these effects, in particular for C8, C8<sup>1</sup>, and C8<sup>2</sup>, reflect conformational changes of the aliphatic side chains of the macrocycle enforced by interactions with the protein. The  $\Delta\delta$  values of  $-2.7$  and  $-3.3$  ppm for the carbons C12<sup>1</sup> of the B850 cofactors are anomalously large. X-ray shows that that both B850 C12<sup>1</sup> carbons are located above the adjacent B850 macrocycle. However, this leads to somewhat smaller  $\sigma^R$  values of  $-1.25$  and  $-2.04$  ppm (Table 1). The imidazole rings of the coordinating histidines also induce a local magnetic field, which can produce a small additional ring current effect of  $\sim -0.5$  ppm on the C12<sup>1</sup> carbons. However, this does not fully explain the total  $\Delta\delta$  for C12<sup>1</sup>.<sup>40</sup>

## Conclusions

Isotropic chemical shift assignments have been obtained for the B800 and B850 cofactors in the LH2 transmembrane protein complex to resolve their molecular electronic structures with atomic selectivity. Three resonance sets from the B800 and two B850 cofactors were extracted selectively from the spectrum of the uniformly [<sup>13</sup>C, <sup>15</sup>N]-labeled LH2 complex isolated from *Rps. acidophila* strain 10050. The NMR dataset of B800 was selectively and unambiguously assigned with the help of a reconstituted U-[<sup>13</sup>C, <sup>15</sup>N]-B800 LH2 complex.

Isotropic chemical shift datasets obtained from the solid-state NMR spectra indicate different chemical environments for each cofactor species. After the isotropic shifts for the ring currents were corrected for in the B850 cofactors, the differences between the three cofactors are small and reveal electronic similarity between B800,  $\alpha$ B850, and  $\beta$ B850 cofactors. All three species show a similar polarization of the long axis of the bacteriochlorin

ring parallel to the Q<sub>y</sub> transition dipole moment. This contrasts with the special pair in the reaction centers of *Rb. sphaeroides*, where convincing evidence was provided for an asymmetric electronic structure of the BChls in the special pair in the reaction center.<sup>8</sup> A similar electronic dipole for both the B800 and the B850 species is detected by NMR, which leads to the conclusion that only a part of the red shift of the B850 cofactors,  $\sim 30$  nm, may be attributed to the protein environment. The large additional red shift of the Q<sub>y</sub> absorption band of B850 with respect to the Q<sub>y</sub> absorption band of B800 is mainly due to overlap between the B850 bacteriochlorin rings in the LH2 protein complex.

We report the observation of electronic charge polarization mainly along the long axis of the  $\pi$ -bonding system as a collective effect of the synergistic contributions of the polar moieties in the cofactor environment. Because shift effects are distributed over the bacteriochlorin ring, rather than localized on specific carbon positions, the induced polarization is attributed to mutual polarization between the cofactors and the protein in a nonlinear dielectric response mechanism. A global collective molecular electronic response, rather than specific localized effects, is in line with theoretical studies that point out the importance of the dielectrics for the protein interior.<sup>32</sup>

**Acknowledgment.** This research was supported in part by demonstration Project B104-CT97-2101 of the commission of the European Communities. H.J.M.d.G. is a recipient of the PIONEER award of the chemical sciences section of The Netherlands Organization for scientific research (NWO). We thank I. de Boer and A. Karawajczyk for their help in using the Gaussian program,<sup>20</sup> and P. Gast and D. de Wit from the Leiden Institute of Physics for the use of the protein preparation facility. Dr. T. J. Aartsma from the Leiden Institute of Physics is gratefully acknowledged for valuable discussions and careful reading of the manuscript. R.J.C. thanks the BBSRC for funding, and N.J.F. was supported by the Gatsby Foundation.

(40) Giessner-Prettre, C.; Pullman, B. *J. Theor. Biol.* **1971**, *31*, 287–294.